

Endostatin, an antiangiogenic drug, induces tumor stabilization after chemotherapy or anti-CD20 therapy in a NOD/SCID mouse model of human high-grade non-Hodgkin lymphoma

Francesco Bertolini, Lisa Fusetti, Patrizia Mancuso, Alberto Gobbi, Chiara Corsini, Pier Francesco Ferrucci, Giovanni Martinelli, and Giancarlo Pruneri

Both chemotherapy and chimeric anti-CD20 monoclonal antibodies are effective agents against B-cell non-Hodgkin lymphoma (NHL). However, patients achieving remission are at risk of relapse. To evaluate the effect of the antiangiogenic drug endostatin used alone and after the administration of cyclophosphamide (CTX) or the anti-CD20 antibody rituximab, we generated a new model of human NHL by transplanting Namalwa cells intraperitoneally into nonobese diabetic/severe combined immunodeficient (NOD/SCID) mice. First, we determined the most effective treatment schedule for the drugs assessed. When administered alone, CTX (3 courses of 75 mg/kg of

body weight given intraperitoneally), rituximab (3 courses of 25 mg/kg given intraperitoneally), and endostatin (5 courses of 50 μ g given subcutaneously) delayed tumor growth, and CTX was the most effective in controlling bulky disease. When given after chemotherapy or immunotherapy, endostatin effectively induced tumor stabilization. When mice given CTX or rituximab on days 3, 5, and 7 after transplantation were randomly assigned to receive endostatin or phosphate-buffered saline on days 15 to 19, tumor growth was prevented in endostatin-treated mice as long as the drug was administered. Furthermore, administration of endostatin on days 25 to 29

after tumor regrowth still induced significant tumor regression, whereas CTX and rituximab were not effective. The specific antiangiogenic action of endostatin was confirmed by *in vitro* and *in vivo* studies indicating that the drug inhibited proliferation and induced apoptosis of endothelial (but not of NHL) cells. In conclusion, sequential administration of chemotherapy and endostatin seems promising for treating bulky NHL, and the less toxic sequential administration of rituximab and endostatin is promising for treating limited disease. (*Blood*. 2000;96:282-287)

© 2000 by The American Society of Hematology

Introduction

Despite recent advances in the treatment of B-cell non-Hodgkin lymphoma (NHL) and the introduction into mainstream hematology-oncology of the chimeric anti-CD20 antibody rituximab, approximately one half of patients with NHL who achieve partial or complete remission after chemotherapy or immunotherapy do relapse.¹ Because the growth of most types of cancers,² possibly including hematologic malignancies,³⁻⁵ depends on the generation of new blood vessels, it was proposed that antiangiogenic therapy may induce solid-tumor dormancy or stabilization.² Preclinical studies of antiangiogenic therapy in nonhematologic malignancies confirmed this hypothesis.⁶ Moreover, the antiangiogenic drug thalidomide was found to be effective in patients with refractory myeloma, another B-cell malignancy.⁷ In addition, a new generation of antiangiogenic drugs was determined to be significantly more effective than thalidomide in inhibiting the growth of endothelial cells.² We generated a novel murine model of human B-cell NHL to evaluate the effect of the new antiangiogenic drug endostatin⁸ used alone and sequentially after chemotherapy or immunotherapy.

Mice bearing the nude or severe combined immunodeficient (SCID) mutation have been used extensively to evaluate human malignancies *in vivo*. However, these strains have residual immunity that may limit posttransplantation neoplastic cell growth, and

evidence has indicated that the nonobese diabetic/SCID (NOD/SCID) strain is more convenient for human leukemia and lymphoma xenotransplantation.⁹⁻¹¹ With the aim of generating a disease similar to human high-grade B-cell NHL, we used intraperitoneal instead of subcutaneous transplantations in NOD/SCID mice and found that Namalwa cells generated intraperitoneal tumors in the injection site. These tumors could be precisely measured with calipers to evaluate the efficacy of different therapies.

Materials and methods

Cell lines and *in vitro* studies of endostatin

The Namalwa cell line (phenotype CD3⁻, CD10⁺, CD13⁻, CD19⁺, CD20⁺, GlyA⁻) derives from an Epstein-Barr virus-positive Burkitt NHL. It was obtained from the American Type Culture Collection (Manassas, VA) and cultured in RPMI and 8% fetal bovine serum (FBS; HyClone, Logan, UT). Human umbilical vein endothelial cells (HUVEC) were obtained from Cascade Biologics (Portland, OR) and cultured in medium 200 (Cascade Biologics) supplemented with 2% FBS and 10 ng/mL each of vascular endothelial growth factor (VEGF) and basic fibroblast growth factor (b-FGF; Peprotech, Rocky Hill, NJ). Human recombinant endostatin

From the Divisions of Hematology-Oncology, Experimental Oncology, and Pathology-Laboratory Medicine, IRCCS European Institute of Oncology, Milan, Italy.

Submitted December 30, 1999; accepted February 24, 2000.

F.B. is a scholar of the US National Blood Foundation.

Reprints: Francesco Bertolini, Hematology-Oncology Unit, European Institute of Oncology, via Ripamonti 435, 20141 Milan, Italy; e-mail: f.bertolini@agora.stm.it.

The publication costs of this article were defrayed in part by page charge payment. Therefore, and solely to indicate this fact, this article is hereby marked "advertisement" in accordance with 18 U.S.C. section 1734.

© 2000 by The American Society of Hematology

produced in *Pichia pastoris* was obtained from Calbiochem (San Diego, CA). In accordance with the findings of O'Reilly et al,⁸ endostatin activity was tested in vitro on HUVEC and Namalwa cells at concentrations ranging from 250 to 1000 ng/mL.

Animal studies

Our model of high-grade human NHL was generated by injecting 6- to 8-week-old NOD/SCID mice intraperitoneally with 10×10^6 Namalwa cells. The mice were evaluated for tumor growth every other day. Tumor volume was measured with calipers, and the formula, $\text{width}^2 \times \text{length} \times 0.52$, was applied to approximate the volume of a spheroid, as described previously.⁶ Injections of treatment agents were given in a site remote from the inoculated tumor. Cyclophosphamide (CTX; Sigma, St Louis, MO) and the chimeric anti-CD20 monoclonal antibody rituximab (Roche, Monza, Italy) were given intraperitoneally, whereas endostatin was given subcutaneously. Control mice received intraperitoneal or subcutaneous injections of phosphate-buffered saline (PBS). Tumor-bearing mice were killed by carbon dioxide asphyxiation, and tumor engraftment was confirmed by histologic, immunohistochemistry (IHC), and flow cytometry (FC) studies. All procedures involving animals were done in accordance with national and international laws and policies.

For histologic and IHC evaluations, tumor samples were fixed in 10% formalin and embedded in paraffin. Then, 4- μm -thick sections were stained with hematoxylin and eosin and with Giemsa stain for conventional histologic assessment. For IHC, sections were immunostained with anti-CD10 and anti-CD20 monoclonal antibodies (DAKO, Glostrup, Denmark). Tumor expression of human CD19 and CD20 antigens was evaluated by FC using monoclonal antibodies from Becton Dickinson (Mountain View, CA). Tumor angiogenesis was evaluated by FC using a new monoclonal antibody (Pharmingen, San Diego, CA) against murine FLK, a VEGF-related receptor found on endothelial cells. Fresh tumors were dissolved at the single-cell level, and 500 to 1000 $\times 10^3$ cells were incubated at 22°C for 30 minutes in PBS and 1% bovine serum albumin with monoclonal antibodies. The percentage of stained cells was determined in comparison with an isotypic control by using a fluorescence-activated cell sorter (FACScalibur; Becton Dickinson). A portion of each sample was incubated with the appropriate isotype control antibodies to establish the background level of nonspecific staining, and positivity was defined as staining greater than nonspecific background staining. To identify apoptotic and dead cells, 7-amino actinomycin D (7AAD) was used as described previously.¹²

Statistical analysis

Statistical comparisons were done with *t* tests and analysis of variance when data were normally distributed. Nonparametric Spearman and Mann-Whitney analyses were used when data were not normally distributed. *P* values lower than 0.05 were considered to represent significance.

Results

After intraperitoneal injection of 10×10^6 Namalwa cells, measurable tumors developed in the injection site in all mice given the transplants (in the middle of the right posterior quadrant of the abdomen; Figure 1). Tumors grew as solid masses in the peritoneal cavity that infiltrated the peritoneum of the abdominal wall. In a few cases, infiltration of the small and large bowel also occurred. Tumors were composed of large cells growing in a diffuse pattern, with round or slightly convoluted nuclei, at least 1 eosinophilic nucleolus, and a thin rim of basophilic cytoplasm. A few larger cells with 2 or more nuclei were also present. Apoptotic bodies were observed frequently, and larger areas of necrosis were also detectable. Scattered among the neoplastic cells were a few histiocytes, although a "starry-sky" pattern was not evident. Visible and measurable tumors were observed beginning on day 10 after transplantation. When left untreated, tumors reached a volume of approximately 5000 mm³ by day 20 (Figures 2-9). This pattern

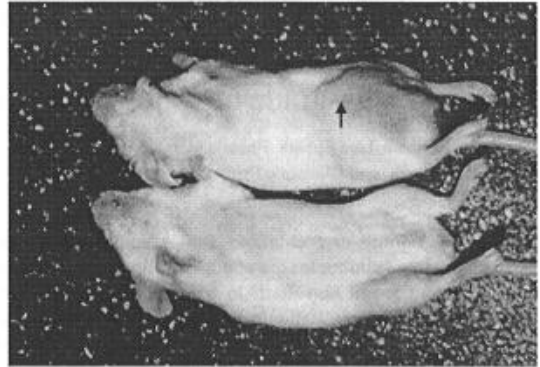


Figure 1. Namalwa tumor growth in nonobese diabetic-severe combined immunodeficient (NOD/SCID) mice given transplants of 10×10^6 cells intraperitoneally. A control mouse is shown on the bottom. The tumor growing in the injection site (arrow) is visible and measurable in the mouse that had transplantation (top).

of tumor growth was similar to that previously described in a subcutaneous model of Namalwa cell xenotransplantation.¹⁰ In the first 30 days after transplantation, tumor metastasis in sites other than the injection site was not observed. In some mice that were given transplants and not treated, metastasis to regional lymph nodes and multiple visceral organs was observed during the second month after transplantation.

CTX, rituximab, and endostatin used as single agents

We first determined the most appropriate treatment schedule for rituximab, CTX, and endostatin used as single agents ($n = 4-10$ animals per group). In our NOD/SCID mouse model, the maximum

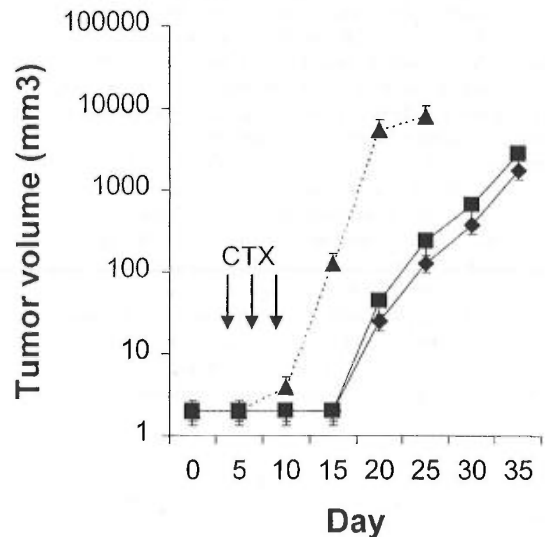


Figure 2. Results of treatment with 2 different doses of cyclophosphamide (CTX). NOD/SCID mice given transplants of 10×10^6 Namalwa cells intraperitoneally were treated with either 150 mg/kg of body weight of CTX or 75 mg/kg of CTX on days 3, 5, and 7. When 150 mg/kg of CTX was administered (\diamond , $n = 10$), 60% of the mice died of drug-related toxicity. When 75 mg/kg of CTX was given (\blacksquare , $n = 10$), none of the mice died of drug-related toxicity, and the delay in tumor growth was not significantly different than at the higher dose. The dotted line indicates tumor growth in 6 untreated controls (\blacktriangle). Results are mean \pm SD values for tumor volume.

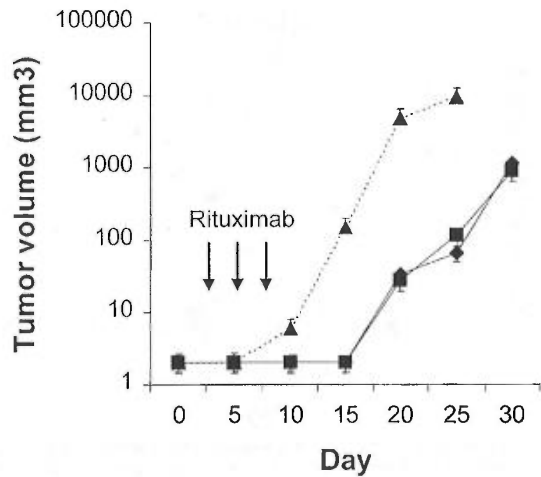


Figure 3. Results of treatment with 2 different doses of rituximab. NOD/SCID mice given transplants of 10×10^6 Namalwa cells intraperitoneally were treated with 75 mg/kg (\blacklozenge) or 25 mg/kg (\blacksquare) of rituximab. Delay in tumor growth was not significantly different in mice given 75 mg/kg of rituximab and those given 25 mg/kg on days 3, 5, and 7 ($n = 4$ per group). The dotted line indicates tumor growth in untreated controls (\blacktriangle). Results are mean \pm SD values for tumor volume.

tolerable dose of CTX was found to be 75 mg/kg per body weight given on days 3, 5, and 7. This treatment significantly delayed tumor growth, and dose escalation to 150 mg/kg killed 60% of the treated mice while not producing a significantly greater response (Figure 2). Three courses of 25 mg/kg of rituximab given on days 3, 5, and 7 were found to delay Namalwa tumor growth, and dose escalation (up to 75 mg/kg) did not produce an additional benefit (Figure 3). Interestingly, when we evaluated the effect of CTX and rituximab on bulky disease by administering these drugs on days 15, 17, and 19 after transplantation, we found that CTX induced a transient reduction in tumor burden, whereas rituximab was not effective

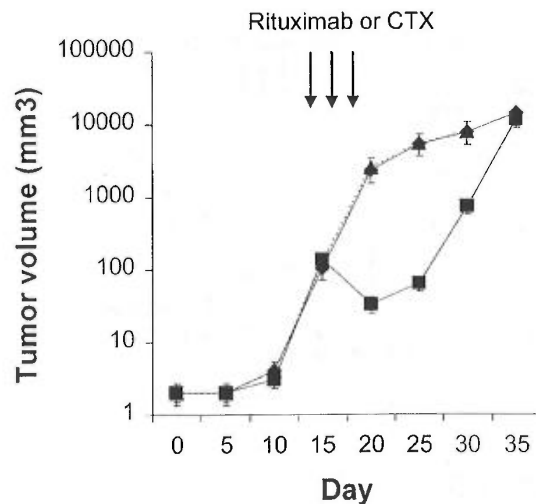


Figure 4. Treatment of bulky disease with CTX (75 mg/kg) or rituximab (25 mg/kg). NOD/SCID mice ($n = 4$ per treatment group) that received transplants of 10×10^6 Namalwa cells intraperitoneally were treated on days 15, 17, and 20 after transplantation. CTX (\blacksquare) induced a significant but transient reduction in tumor burden, whereas rituximab (\blacklozenge) did not. The dotted line indicates tumor growth in untreated controls (\blacktriangle). Results are mean \pm SD values for tumor volume.

(Figure 4). For endostatin, our in vitro studies indicated that 250 to 1000 ng/mL of this agent inhibited 34% to 66% of HUVEC proliferation, whereas no effect was observed on Namalwa cell proliferation ($P < .001$; Figure 5A). In vivo, 5 courses of 50 μ g endostatin given on days 3 to 7 significantly delayed tumor growth (Figure 5B).

CTX, rituximab, and endostatin used sequentially

Four to 6 animals per group were evaluated in sequential-administration studies. When given after CTX or rituximab,

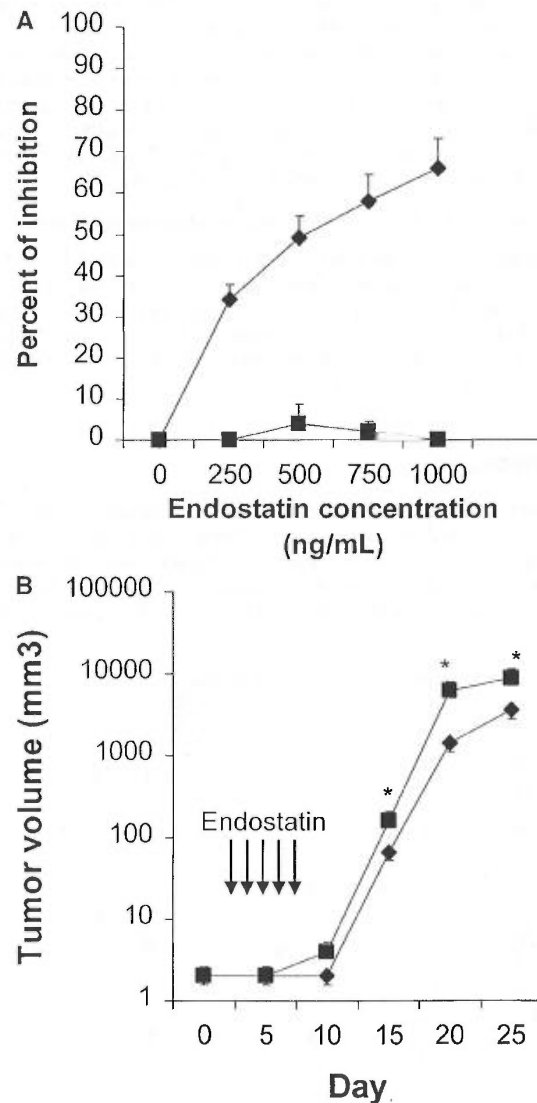


Figure 5. Results of in vitro and in vivo studies of endostatin. (A) Specific inhibition of human umbilical vein endothelial cells (HUVEC) (\blacklozenge) by endostatin. HUVEC were cultured in medium 200 supplemented with 10 ng/mL vascular endothelial growth factor and basic fibroblast growth factor. Namalwa cells (\blacksquare) were cultured in RPMI-8% fetal bovine serum in a 72-hour proliferation assay.⁸ Endostatin inhibited proliferation of HUVEC but not Namalwa cells in a dose-dependent fashion. Results are mean \pm SD values ($n = 3$). (B) Endostatin treatment (\blacklozenge , 50 μ g per mouse on days 3 to 7) significantly delayed tumor growth in NOD/SCID mice given transplants of 10×10^6 Namalwa cells intraperitoneally. The dotted line indicates tumor growth in untreated controls (\blacksquare). Results are mean \pm SD values for tumor volume ($n = 4$ per group). * $P < 0.01$.

endostatin effectively induced tumor stabilization. As shown in Figure 6, mice given 3 courses of rituximab on days 3, 5, and 7 after transplantation were randomly assigned to receive 50 µg of endostatin or PBS on days 15 to 19. In endostatin-treated mice, but not in PBS-treated mice, tumor growth was prevented as long as the endostatin was administered. Endostatin was similarly effective in mice given 3 courses of CTX on days 3, 5, and 7 after transplantation and randomly assigned to receive 50 µg of endostatin or PBS on days 15 to 19 (Figure 7). It is noteworthy that administration of endostatin on days 25 to 29 after tumor regrowth still induced significant tumor regression ($P = .02$ by paired t test; Figure 7). Conversely, when rituximab was administered after CTX, it delayed tumor growth in comparison with results in PBS-treated controls but did not prevent tumor growth or induce a significant tumor regression after tumor regrowth (Figure 8). Similarly, when CTX was administered after rituximab, tumor growth was delayed in comparison with results in PBS-treated controls, but neither prevention of tumor growth nor regression after tumor regrowth was observed (Figure 9).

Induction of in vivo endothelial cell apoptosis by endostatin

Figure 10 shows the frequency of apoptosis in endothelial cells from dissolved Namalwa tumors. As indicated by double staining for murine FLK and 7AAD, 8.3% ± 1.9% of endothelial cells from endostatin-treated animals were apoptotic. This value was 4 times higher than that in control mice given PBS, CTX, or rituximab (1.7% ± 1.1%; $P > .001$).

Discussion

Studies using preclinical models of nonhematologic malignancies have indicated that antiangiogenic therapies may delay or even abrogate tumor growth.^{2,6,8} Moreover, several findings suggest that angiogenesis may be clinically relevant in hematopoietic malignancies,³⁻⁵ and the antiangiogenic drug thalidomide has been found to

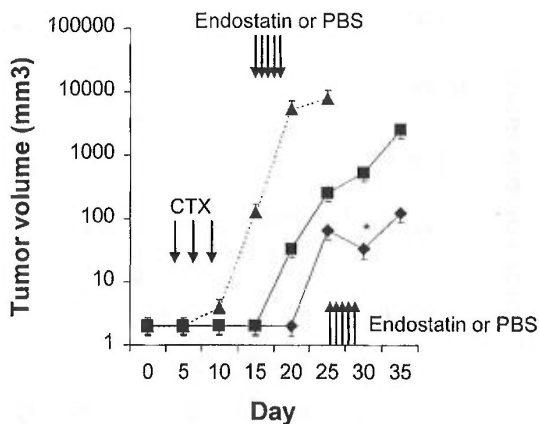


Figure 7. Results with CTX followed by endostatin. NOD/SCID mice that received transplants of 10×10^6 Namalwa cells intraperitoneally were given 3 courses of CTX (75 mg/kg) on days 3, 5, and 7 after transplantation and randomly assigned to receive 50 µg of endostatin (◆) or PBS (■) on days 15 to 19. In endostatin-treated mice, but not in PBS-treated mice, tumor growth was prevented as long as endostatin was administered. Moreover, administration of endostatin on days 25 to 29 after tumor regrowth induced significant tumor regression ($P = .02$ by paired t test comparing tumor volume on day 25 with that on day 30). The dotted line indicates tumor growth in untreated controls (▲). Results are mean ± SD values for tumor volume ($n = 6$ per group). * $P = .02$ vs day 25.

be effective in patients with multiple myeloma refractory to chemotherapy.⁷ Furthermore, thalidomide also seems to be effective in myelodysplastic syndromes, myeloproliferative disorders, and myelofibrosis.^{13,14} All these hematologic diseases, including myeloma, are associated with relevant bone marrow angiogenesis.^{4,5} We and others¹⁵⁻¹⁸ have investigated the role of angiogenesis and angiogenic growth factors in NHL. Expression of VEGF and related receptors Flt-1 and FLK-KDR has been observed in most B-cell hematopoietic malignancies,¹⁷ and the autocrine and paracrine roles of this growth factor are being evaluated. In addition, remodeling and immature vessels were observed in biopsy

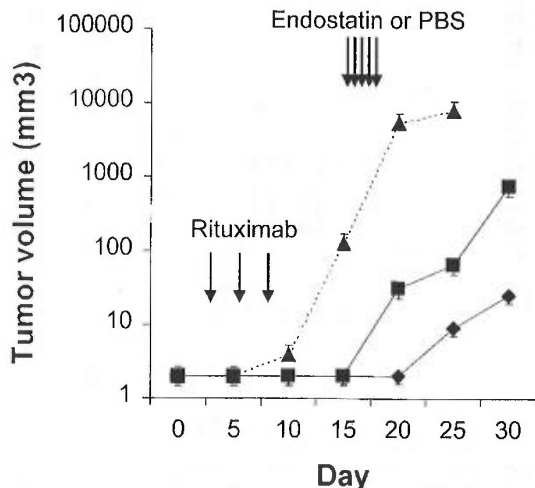


Figure 6. Results of treatment with rituximab followed by endostatin. NOD/SCID mice that received transplants of 10×10^6 Namalwa cells intraperitoneally were given 3 courses of rituximab (25 mg/kg) on days 3, 5, and 7 after transplantation and randomly assigned to receive 50 µg of endostatin (◆) or phosphate-buffered saline (PBS) (■) on days 15 to 19. In endostatin-treated mice, but not in PBS-treated mice, tumor growth was prevented as long as endostatin was administered. The dotted line indicates tumor growth in untreated controls (▲). Results are mean ± SD values for tumor volume ($n = 4$ per group).

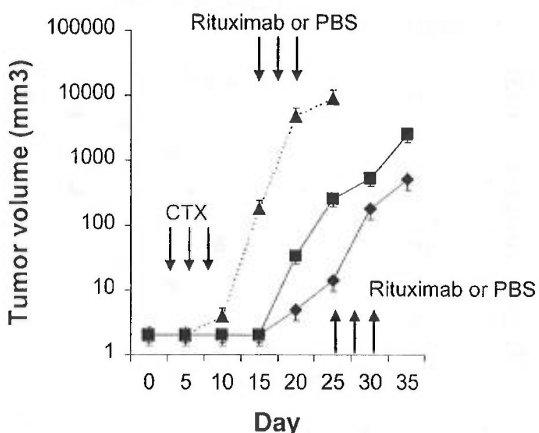


Figure 8. Results with CTX followed by rituximab. NOD/SCID mice that received transplants of 10×10^6 Namalwa cells intraperitoneally were given 3 courses of CTX (75 mg/kg) on days 3, 5, and 7 after transplantation and randomly assigned to receive 25 mg/kg of rituximab or PBS on days 15, 17, and 19 (first course) and on days 25, 27, and 29 (second course). Rituximab (◆) delayed tumor growth in comparison with results in PBS-treated controls (■) but did not prevent tumor growth or induce significant tumor regression after tumor regrowth. The dotted line indicates tumor growth in untreated controls (▲). Results are mean ± SD values for tumor volume ($n = 4$ per group).

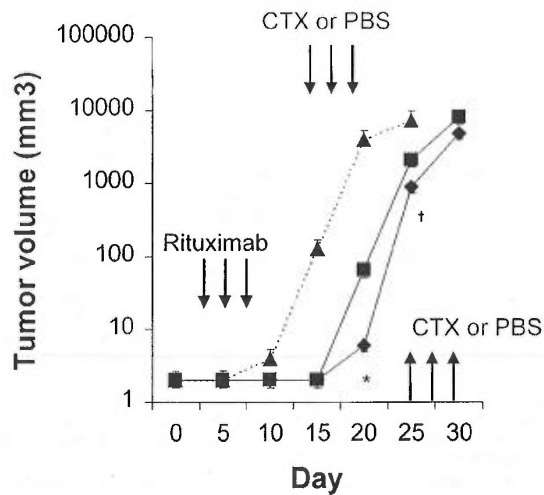


Figure 9. Results with rituximab followed by CTX. NOD/SCID mice that received transplants of 10×10^6 Namalwa cells intraperitoneally were given 3 courses of rituximab (25 mg/kg) on days 3, 5, and 7 after transplantation and randomly assigned to receive 75 mg/kg CTX (\blacklozenge) or PBS (\blacksquare) on days 15, 17, and 19 (first course) and on days 25, 27, and 29 (second course). CTX delayed tumor growth in comparison with results in PBS-treated controls but did not prevent tumor growth or induce significant tumor regression after tumor regrowth. The dotted line indicates tumor growth in untreated controls (\blacktriangle). Results are mean \pm SD values for tumor volume ($n = 4$ per group). * $P = .003$; † $P = .02$.

specimens of high-grade NHL (F. Pezzella, unpublished data), and high circulating levels of VEGF and b-FGF (the other endothelial cell mitogenic factor) were found to correlate with a poor prognosis in patients with NHL.^{15,16,18}

When generating animal models of human cancer, it is important to consider that tumor angiogenic phenotype can be modulated by cytokines released by host cells in specific microenvironments. Human renal cancer cells, for instance, express high levels of the angiogenic growth factor b-FGF when growing in kidney, but not when growing subcutaneously.¹⁹ Thus, we reasoned that an intraperitoneal tumor model was more appropriate than a subcutaneous model for evaluating the effect of endostatin in B-cell NHL. By using NOD/SCID mice given transplants of Namalwa cells, we generated a reliable *in vivo* model of aggressive intraperitoneal human B-cell

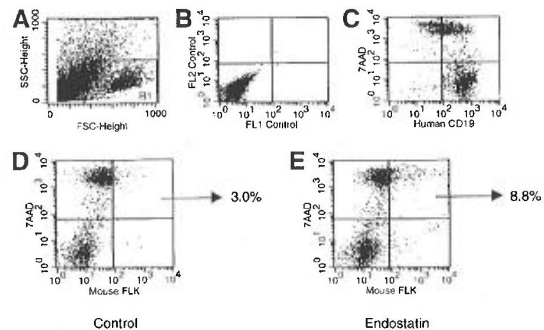


Figure 10. Representative dot plots indicating the frequency of endothelial cell apoptosis in Namalwa tumors generated in NOD/SCID mice. Tumors dissolved as single cells were evaluated by flow cytometry. Panel A shows forward and side scatters of the cell suspension and the analysis gate, panel B the negative control, and panel C the human CD19⁺ phenotype of the tumor. As indicated by the percentage of murine cells positive for FLK and 7-amino actinomycin D (panels D and E), the frequency of endothelial apoptotic cells was significantly increased in mice given endostatin.

NHL that allows measurement of tumor, closely resembles the human disease, and has 100% engraftment efficiency. In fact, the animal model described in this study was similar to human Burkitt NHL, a B-cell malignancy that, in most endemic and sporadic cases, affects abdominal viscera. The model had 100% engraftment efficiency: measurable intraperitoneal tumors developed in the injection site in all mice given transplants. Remarkably, the Namalwa line was previously found to be the most aggressive in a panel of lymphoid lines tested in subcutaneous xenotransplant studies.¹⁰

To study the efficacy of endostatin used alone and in combination with established chemotherapy and immunotherapy protocols in our NHL model, we chose drug-administration schedules in accordance with previously published information.¹ When seeking the most effective dosages of CTX and rituximab, we found that toxicity limited CTX administration and that drug resistance was progressively acquired. Rituximab efficiency reached a plateau at a dose of 25 mg/kg, and in our model, as well as in NHL patients (F. Pezzella et al, unpublished data), this agent was less active than CTX in cases of bulky disease. To our knowledge, our study is the first to indicate that rituximab is effective in NOD/SCID mouse models of human B-cell NHL. The evidence that rituximab was active *in vivo* against human NHL, despite the fact that the host mice had a severe deficiency of B cells, T cells, natural killer cells, myeloid cells, and complement,¹¹ is of particular interest. In fact, it suggests that at least some of rituximab-induced biologic responses may not be due to antibody-dependent cellular cytotoxicity or complement-dependent cell lysis.

Endostatin is one of the more promising antiangiogenic drugs, and our *in vitro* data indicate that it has a direct effect on newly generated endothelial cells without producing a detectable effect on NHL cells. Our study indicates that sequential administration of endostatin after rituximab or CTX effectively induces tumor stabilization. It should be noted that in mice treated in the first week after tumor transplantation, sequential administration of the nontoxic drugs rituximab and endostatin was at least as effective as sequential administration of CTX (a highly toxic drug) and endostatin. Our data also confirm the results of a study⁶ in mice treated for 240 to 320 days with multiple cycles of high-dose endostatin that indicated that this antiangiogenic drug, in sharp contrast to chemotherapy drugs such as CTX, does not induce acquired drug resistance.

On the other hand, long-term administration of endostatin is needed because tumor relapse has been observed after discontinuation of the drug. The ultimate goal of antiangiogenic therapy is to induce long-term tumor stabilization.²⁰ Because data from studies in nonhuman primates have indicated that endostatin may be administered for long periods without producing toxicity,²¹ we suggest that this agent might be evaluated in clinical trials as a consolidation drug for patients who have achieved remission. The data we obtained by using our murine model indicate that sequential administration of chemotherapy and endostatin seems appropriate in patients with bulky disease, whereas the less toxic sequential administration of rituximab and endostatin seems effective in patients with limited disease. In this context, B-cell malignancies are of particular interest because molecular probes for quantifying minimal residual disease in blood and bone marrow are available for most patients.

Acknowledgments

We thank Francesco Pezzella, Domenico Delia, Carmelo Carlo-Stella, and Davide Soligo for critical reading of the manuscript.

Explore Litigation Insights

Docket Alarm provides insights to develop a more informed litigation strategy and the peace of mind of knowing you're on top of things.

Real-Time Litigation Alerts



Keep your litigation team up-to-date with **real-time alerts** and advanced team management tools built for the enterprise, all while greatly reducing PACER spend.

Our comprehensive service means we can handle Federal, State, and Administrative courts across the country.

Advanced Docket Research



With over 230 million records, Docket Alarm's cloud-native docket research platform finds what other services can't. Coverage includes Federal, State, plus PTAB, TTAB, ITC and NLRB decisions, all in one place.

Identify arguments that have been successful in the past with full text, pinpoint searching. Link to case law cited within any court document via Fastcase.

Analytics At Your Fingertips



Learn what happened the last time a particular judge, opposing counsel or company faced cases similar to yours.

Advanced out-of-the-box PTAB and TTAB analytics are always at your fingertips.

API

Docket Alarm offers a powerful API (application programming interface) to developers that want to integrate case filings into their apps.

LAW FIRMS

Build custom dashboards for your attorneys and clients with live data direct from the court.

Automate many repetitive legal tasks like conflict checks, document management, and marketing.

FINANCIAL INSTITUTIONS

Litigation and bankruptcy checks for companies and debtors.

E-DISCOVERY AND LEGAL VENDORS

Sync your system to PACER to automate legal marketing.